

Observation of Proximity Resonances in a Parallel-Plate Waveguide

J. S. Hersch^{1,*} and E. J. Heller^{1,2,†}

¹*Department of Physics, Harvard University, Cambridge, Massachusetts 02138*

²*Harvard-Smithsonian Center for Astrophysics, Cambridge, Massachusetts 02138*

**e.mail: hersch@monsoon.harvard.edu*

†*e.mail: heller@physics.harvard.edu*

Experiments with dielectric scatterers in a parallel-plate waveguide have verified for the first time the existence of proximity resonances in two dimensions. A numerical solution to the scattering problem supports the analysis of the experimental data.

It has recently been shown that two resonant s-wave scatterers placed close together produce two resonances in the spectrum of the combined system [1]. The first, which remains s-wave in character, is shifted down in energy and broadened with respect to the original single scatterer resonance. The second resonance, which is p-wave in character, is shifted up an equal amount in energy and can have a very narrow width. In fact, the width of the p-wave resonance vanishes as the scatterers approach each other. This second resonance has been dubbed the proximity resonance.

Proximity resonances are important in a number of physical contexts, including scattering of sound from small identical bubbles in liquids [2,3], and scattering and emission of light from nearby dipole scatterers [4,5] where a proximity resonance effect has long been known under the name of Dicke super-radiance and sub-radiance. In Ref. [1], the effect was discussed for particle scattering from two identical atoms (or other identical scatterers) for the first time. Here we discuss yet another context, the classical scattering of electromagnetic waves from dielectric discs. At the same time (however see the caveat below) the system we describe mimics quantum scattering from two adjacent potential wells in two dimensions [6,7].

For the purposes of modeling the experiment, we developed a method of solving the scattering problem involving cylindrical basis functions centered on each disc. It turned out that the point scatterer model [8,9], which was used in the original discussion of proximity resonances [1], was not sufficient to accurately model the experiment. In order for the point scatterer model to be applicable, at least two conditions must be met: $r \ll \lambda$, and $r \ll d$, where r is the physical radius of each scatterer, λ the wavelength, and d the distance between the scatterers. In our experiments, the first condition was always met, but the second was not.

Other work [10] indicates that there may be a similar effect present in the bound state spectrum of two nearby dielectric discs in a parallel-plate waveguide. Szymtkowski *et al.* [11] have found theoretically a similar resonance with fixed scattering length point interactions.

The picture to keep in mind when thinking about the proximity resonance is the following: imagine two nearby point sources of unit amplitude, situated much closer together than a wavelength. When these sources are in phase, amplitude will add up nearly in phase everywhere in space, and the amplitude far from the sources will be appreciable. The far field intensity clearly will be s-wave in character. When the sources are out of phase, amplitude will interfere destructively everywhere, and the far field intensity will be much reduced compared to the in-phase case. Now, for a scattering resonance, the width of the resonance is proportional to the rate at which amplitude escapes from the neighborhood of the scattering system. This rate is proportional to the ratio $|\psi_{\text{far}}/\psi_{\text{near}}|^2$, where ψ_{far} is the far field amplitude and ψ_{near} is the amplitude in the near field. This ratio will remain finite for the in-phase pair of scatterers, and vanish for the out of phase pair, as their separation goes to zero. This narrows the proximity resonance as the scatterers are brought closer together.

The waveguide, shown in Fig. 1, consisted of two parallel copper plates, 1 m square, separated by a 1 cm gap. To minimize the effect of waves reflected off the edges of the waveguide, the perimeter was lined with a 11.5 cm thick layer of microwave absorber (C-RAM LF-79, Cuming Microwave Corp.), designed to provide 20 dB of attenuation in the reflected wave intensity at frequencies above 600 MHz. Without the absorber, there would be substantial reflections of both the incident and scattered wave off the edges of the waveguide, which would produce strong cavity modes and unnecessarily complicate the analysis. The important effect of the absorber was to allow the waveguide to behave as if it were infinite in extent in the directions parallel to the plates, and thus support oscillations at all frequencies.

The scatterers were cylindrical in shape (radius: 2 mm, height: 1 cm) and had a measured dielectric constant of $\epsilon = 77 \pm 1$. Each disc had an individual s-wave scattering resonance at 2.3 GHz with a 1.1 GHz width. They were illuminated with microwaves from a point source located 25 cm away from the midpoint of the two scatterers. The field in the waveguide could be measured at eight points located on a circle of 25 cm radius centered at the midpoint between the scatterers.

Antennae were inserted perpendicular to the plates to launch the incident wave and measure the field. Such antennae couple to an electric field perpendicular to the plates. For a plate separation of 1 cm and frequencies below

15 GHz (the experiment operated between 1-3 GHz), *only* the TEM (transverse electromagnetic) mode propagates in the waveguide, and all others are evanescent. The classification TEM means that, for this mode, both \vec{E} and \vec{H} are transverse to the direction of propagation. In particular, \vec{E} is everywhere perpendicular to the plates, and \vec{H} is everywhere parallel to the plates. As an example, we calculate the decay constant, $\kappa = \sqrt{k_z^2 - (\omega/c)^2}$, for the mode with one oscillation transverse to the plates at 3 GHz. With $k_z = \pi/L$ and $L = 1$ cm, we find $\kappa \simeq 3$ cm⁻¹. This means that this mode has decayed by a factor e^{-75} over a distance of 25 cm, the distance between the source and the scatterers. Thus we may safely ignore all modes but the TEM mode for the purpose of this work.

As mentioned above, for the TEM mode both \vec{E} and \vec{H} are transverse to the direction of propagation, just as for a plane wave in free space. In fact, a useful visualization of this mode in the waveguide is just a section of an infinite plane wave, $\vec{E}_0 e^{i\vec{k}\cdot\vec{r}}$, with wave vector \vec{k} parallel, and electric field \vec{E}_0 normal to the plates. Furthermore, the TEM mode has *no variation* of the fields in the direction perpendicular to the plates and is thus truly two dimensional [12]. In fact, the entire field structure $\{\vec{E}(x, y), \vec{H}(x, y)\}$ can be derived from knowledge of $E_z(x, y)$ alone [13], where z is understood to be the direction perpendicular to the plates. Furthermore, for the TEM mode, the boundary conditions on E_z at the dielectric surface are identical to those of a quantum mechanical square well: E_z and its normal derivative, $\partial_n E_z$, must be continuous across the interface. Thus the component E_z in the waveguide plays the role of ψ in a two dimensional quantum mechanical system. Henceforth we will refer to E_z as ψ .

However, there remains one important difference between dielectrics and quantum mechanical square wells. In quantum mechanics, the ratio of wavenumbers inside and outside the well is

$$\frac{k_{\text{in}}}{k_{\text{out}}} = \sqrt{\frac{E - V}{E}},$$

where V is the well depth and E is the energy. Note that this ratio depends on E , and diverges at low energy. In the electromagnetic case, this ratio is a constant, and equal to the index of refraction:

$$\frac{k_{\text{in}}}{k_{\text{out}}} = \sqrt{\epsilon}.$$

This means that a system of quantum square wells can only be compared with an equivalent system of dielectric discs at a particular energy. If the energy is changed, ϵ must also be changed to retain correspondence.

The measured signal was compared to the source signal in both amplitude and phase with a HP 8714C network analyzer. Because both amplitude and phase could be measured, it was possible to extract the (complex) scattered wave, ψ_s from the full signal, $\psi = \psi_0 + \psi_s$, where ψ_0 is the incident wave. This was done by removing the scatterers from the waveguide and repeating the measurement, yielding ψ_0 . This result was then subtracted from the full wave to yield the scattered wave signal.

The full solution to the scattering problem of a single dielectric disc in a parallel plate waveguide can be found analytically [14]. The two disc problem, however, becomes difficult because of the lack of cylindrical symmetry. We address this difficulty by using a basis which reflects the broken symmetry of the problem: two sets of Bessel functions, each centered on one of the discs. This method is similar in spirit to that of Goell [15]. Referring to Fig. 2, we have in regions I, II, and III, respectively,

$$\psi_I = \sum_{l=-l_{\text{max}}}^{l_{\text{max}}} A_l J_l(\kappa r_1) e^{il\theta_1},$$

$$\psi_{II} = \sum_{l=-l_{\text{max}}}^{l_{\text{max}}} B_l J_l(\kappa r_2) e^{il\theta_2},$$

and

$$\psi_{III} = \psi_0 + \sum_{l=-l_{\text{max}}}^{l_{\text{max}}} \left[C_l H_l^{(1)}(\kappa r_1) e^{il\theta_1} + D_l H_l^{(1)}(\kappa r_2) e^{il\theta_2} \right],$$

where $J_l(x)$ and $H_l^{(1)}(x)$ are Bessel functions and Hankel functions of the first kind, ψ_0 is a TEM incident wave, $\kappa = \sqrt{\epsilon} k$, and l_{max} determines the size of the basis set. Note that the variable z does not appear in the above equations, because for the TEM mode there is no z dependence of the fields. An exact solution would require that

$l_{\max} \rightarrow \infty$. However, we find very good solutions for l_{\max} as small as 5. The complex constants A_l, B_l, C_l, D_l are to be determined by matching ψ and its normal derivative $\partial_n \psi$ along the perimeter of each disc.

The exact solution would require matching $\{\psi, \partial_n \psi\}$ at all points along the boundary of each disc. In practice, one can only match at a finite number of points. From each matching point, one obtains two equations relating the constants A_l, B_l, C_l, D_l . The entire collection of matching equations can be expressed in matrix form, $Mx = b$, where the number of rows and columns of M is determined by the number of matching points and basis functions, respectively. The vector x is built up of the coefficients A_l, B_l, C_l, D_l , and b is determined by the incident wave ψ_0 . In general, one chooses more matching points than basis functions, so that the solution x minimizes the length $r = |Mx - b|$. This minimization is efficiently carried out by finding the singular value decomposition of the matrix M [16]. The residual r provides an indication of the accuracy of the solution. For this work, typical values of r were 10^{-10} per matching point. This is to be compared with values of $|\psi|$ and $|\partial_n \psi|$ of order unity on the perimeters of the discs.

In Fig. 3 we plot the scattered amplitude $|\psi_s| = |\psi - \psi_0|$ measured at position 7 (see Fig. 1). The theoretical result agrees very well, apart from a weak 0.3 GHz modulation of the experimental signal due to reflections off the absorbing walls of the waveguide. The numerical data was generated using $l_{\max} = 5$ and matching at 10 equally spaced locations around each disc. The broad feature centered around 2.0 GHz is the s-wave (in phase) resonance. A strong proximity resonance is apparent at around 2.8 GHz. The width of this peak is smaller by a factor of 7 than the single scatterer s-wave resonance width. We also checked that this peak was indeed p-wave in character by measuring the angular dependence of the scattered wave in the vicinity of 2.8 GHz. Notably, the peak was absent when the measuring antenna was placed on the line equidistant from each disc, which defines a nodal line of the scattered wave for a p-wave resonance.

In Figs. 4, 5 we plot the peak position and width, respectively, of the proximity resonance as a function of disc separation. Again the numerical predictions are in good agreement with the data. For comparison, we also include the predictions of the cruder point scatterer model, using as input parameters a single scatterer resonance frequency $f_0 = 2.3$ GHz and width of $\Gamma_0 = 1.1$ GHz. It can be shown that within this model, the proximity resonance peak position f and width Γ obey the following formulae,

$$f = f_0 - \frac{\Gamma_0}{2} Y_0(k_0 d), \quad \Gamma = \Gamma_0 (1 - J_0(k_0 d)),$$

where J_0 is a zeroth order Bessel function, Y_0 is a zeroth order Neumann function, k_0 is the on-resonance wave number of a single scatterer, and d is the distance between the scatterers. The point scatterer model does a good job of tracking the peak positions, but the resonance widths are not described well by the model.

In summary, we have, for the first time, observed proximity resonances in a two dimensional system. The analysis of the experimental data seems to be well supported by a numerical solution to the scattering problem. Immediate extensions of the ideas presented here include increasing the number of scatterers to look for even narrower resonances, which would be associated with higher angular momentum scattered waves (d-waves, for example). The spectrum of a dense (compared to a wavelength), ordered array of s-wave resonant scatterers is also an interesting system as it relates to band structure formation.

We acknowledge S. Sridhar and K. Pance for suggesting the use of high ϵ dielectrics in our experiment. We would like to thank P. Horowitz for advice on microwave techniques, and especially for the use of his network analyzer. J. Doyle provided insight and encouragement. This work was supported through funding from Harvard University, and the National Science Foundation, through ITAMP and also Grant nsf-che9610501.

-
- [1] E. J. Heller, Phys. Rev. Lett. **77**, 4122 (1996).
 - [2] I. Tolstoy, J. Acoust. Soc. Am. **80**, 282 (1986); **83**, 2086 (1988).
 - [3] C. Feuillade, J. Acoust. Soc. Am. **98**, 1178 (1995).
 - [4] R.G. Devoe and R.G. Brewer, Phys. Rev. Lett. **76**, 2049 (1996); R.G. Brewer, Phys. Rev. A **52** (1995).
 - [5] P.R. Berman, Phys. Rev. A, **55** 4466 (1997).
 - [6] S. Sridhar, Phys. Rev. Lett. **67**, 785 (1991).
 - [7] (a) H. J. Stöckman and J. Stein, Phys. Rev. Lett. **64**, 2215 (1990); (b) J. Stein and H. J. Stöckman, Phys. Rev. Lett. **68**, 2867 (1992); (c) S. L. McCall, P.M. Platzman, R. Dalichaouch, D. Smith, and S. Schultz, Phys. Rev. Lett. **67**, 2017 (1992).
 - [8] L. S. Rodberg and R. M. Thaler, *Introduction to the Quantum Theory of Scattering*, (Academic, New York, 1967), p 350.

- [9] G. Drukarev, Adv. Quantum Chem. **11**, 251 (1978).
- [10] S. Sridhar (private communication).
- [11] R. Szmytkowski and C. Szmytkowski, Phys. Lett. A, **235**, 217 (1997).
- [12] S. Sridhar, D. Hogenboom and B. A. Willemsen, J. Stat. Phys. **68**, 239 (1992).
- [13] J. D. Jackson, *Classical Electrodynamics*, (Wiley, New York, 1975), p. 341.
- [14] H. C. van de Hulst, *Light Scattering by Small Particles*, (Wiley, New York, 1957), p. 297. Note that the van de Hulst solution is for scattering off an infinite dielectric cylinder in free space, with arbitrary polarization and direction of the incident wave. If the polarization is taken parallel, and the incident direction normal to the axis of the cylinder, then this solution is exactly analogous to TEM scattering in our waveguide.
- [15] J. E. Goell, Bell Syst. Tech. J. **48**, 2133 (1969).
- [16] W. H. Press, S. A. Teukolsky, W. T. Vetterling, and B. P. Flannery, *Numerical Recipes in C*, (Cambridge University Press, Cambridge, 1992), p. 59.

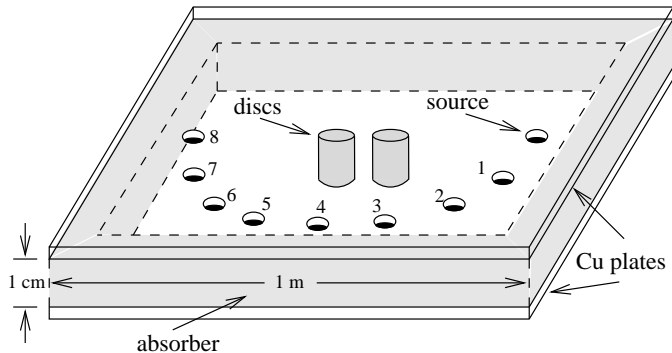


FIG. 1. The scattering arena. Source and receiving antennae were inserted through holes drilled in the top plate. The field could be measured in any of eight locations located on a semicircle 25 cm from the discs. Note that the figure is not drawn to scale.

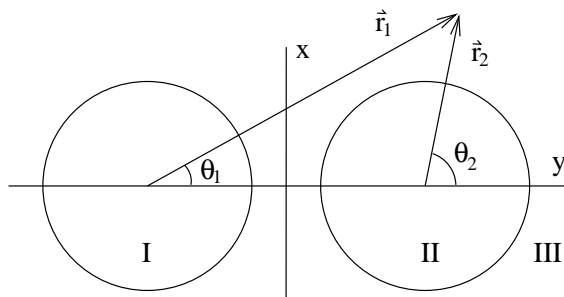


FIG. 2. A coordinate system for two disc scattering.

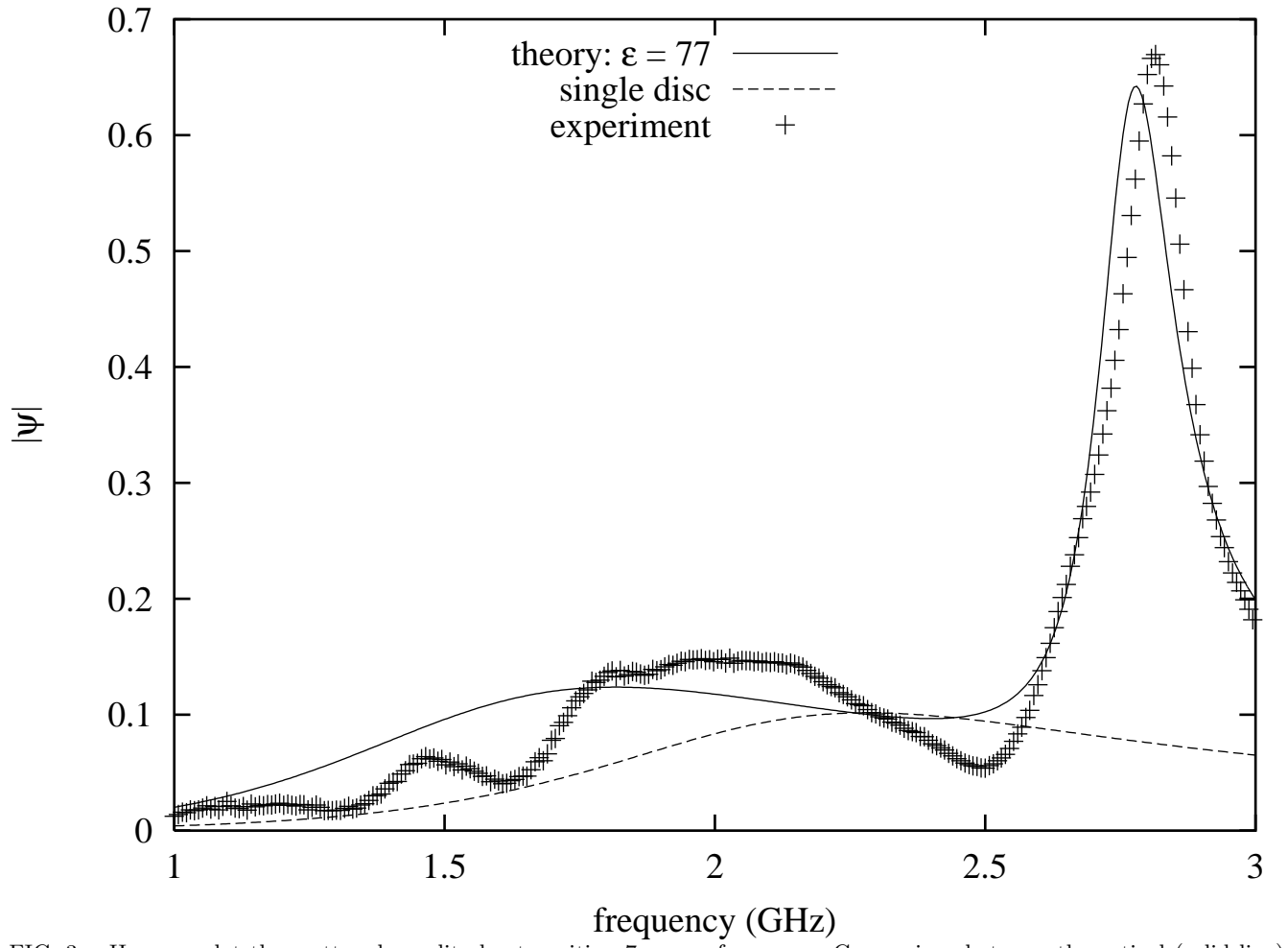


FIG. 3. Here we plot the scattered amplitude at position 7 versus frequency. Comparison between theoretical (solid line) and experimental data (crosses). Disc separation: 1.0 cm. The single disc resonance also shown (dashed line).

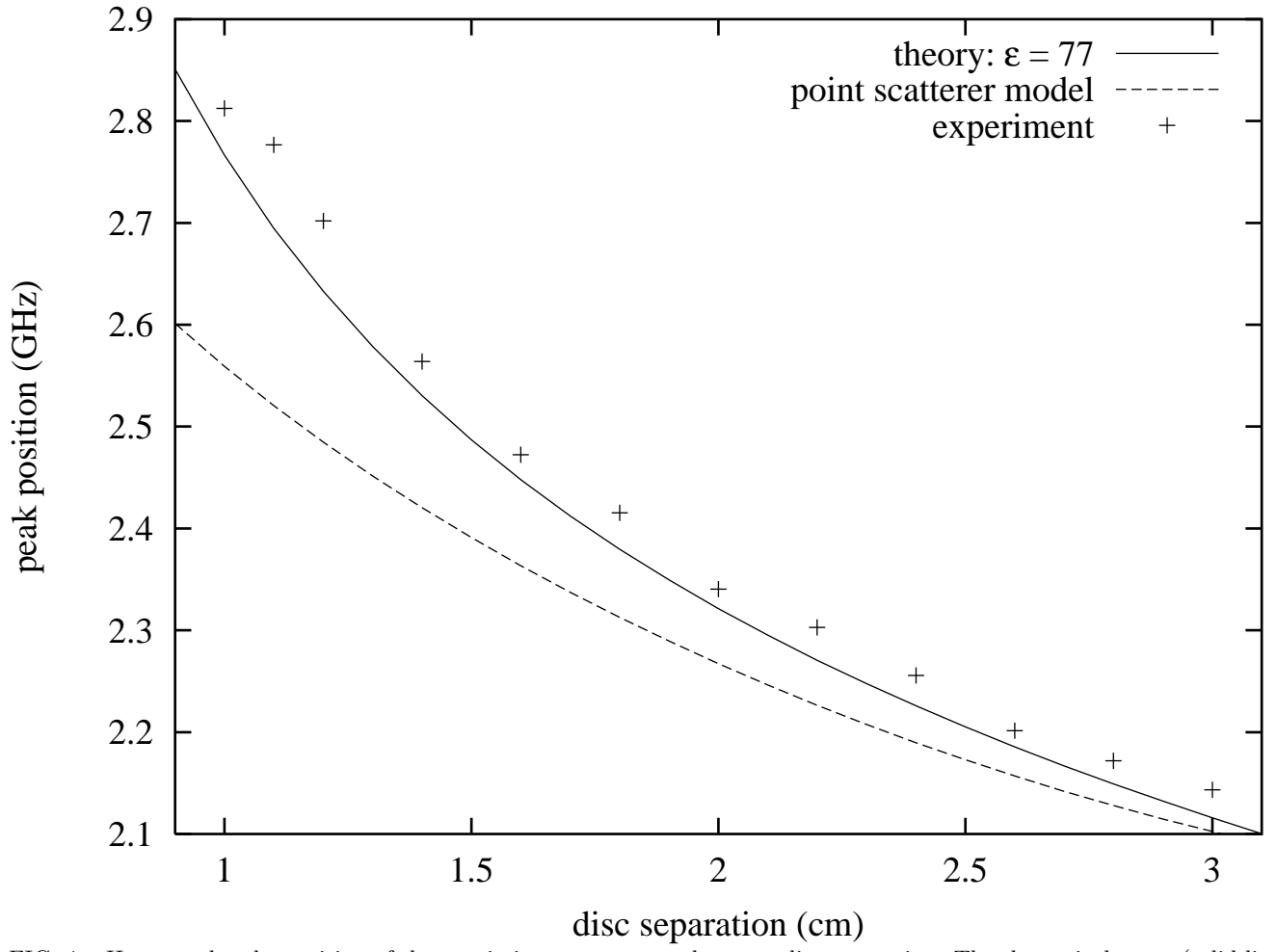


FIG. 4. Here we plot the position of the proximity resonance peak versus disc separation. The theoretical curve (solid line) tracks the experimental values well (crosses). The point scatterer model prediction is also shown (dashed line).

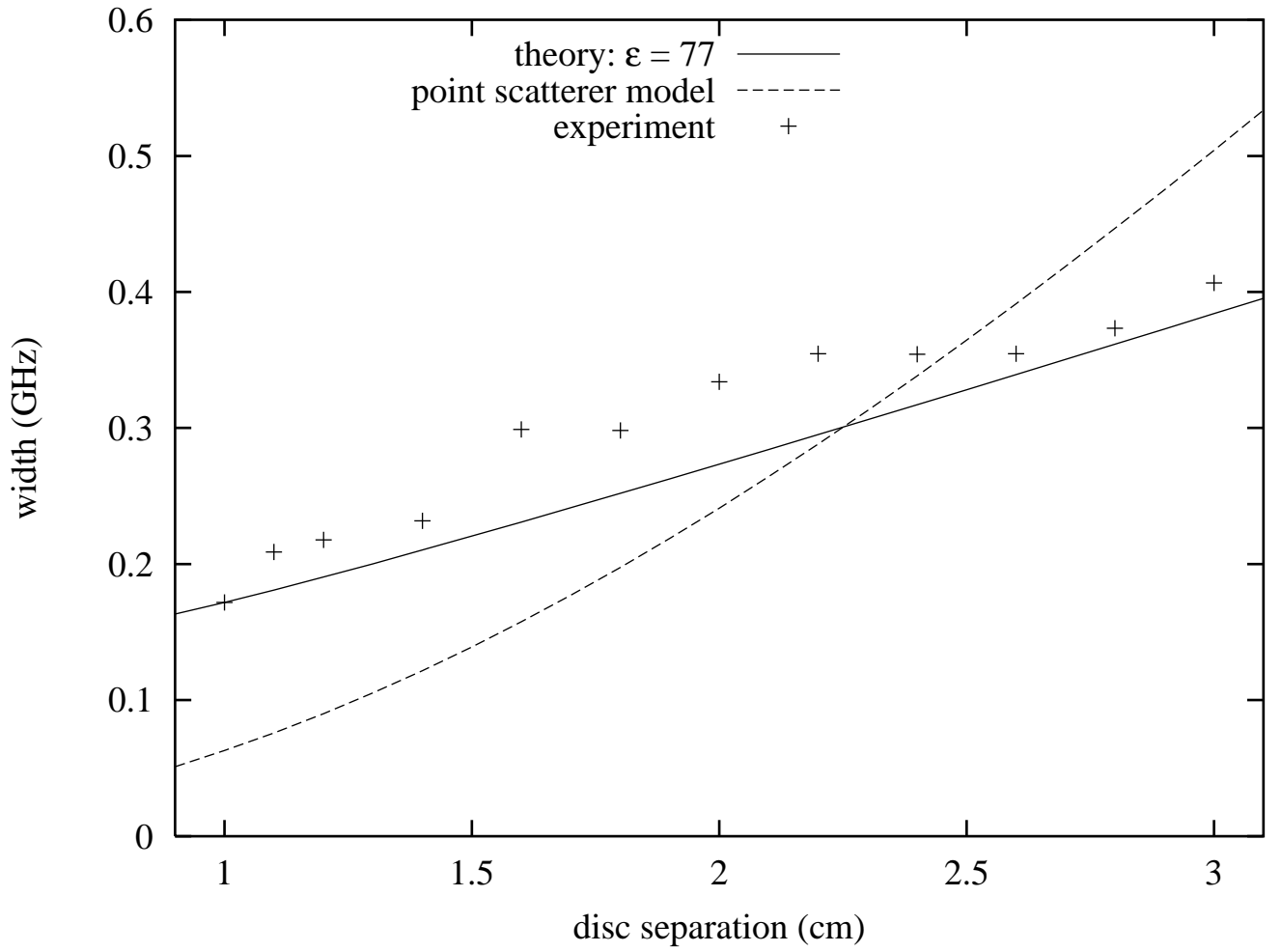


FIG. 5. Here we plot the width of the proximity resonance versus disc separation. As above, the theoretical curve (solid line) models the experimental data (crosses) well. The point scatterer model prediction is also shown (dashed line).